Title

Development and characterization of a novel rat model of type 2 diabetes mellitus: the UC Davis type 2 diabetes mellitus UCD-T2DM rat

Journal

AJP Regulatory Integrative and Comparative Physiology, 295(6)

ISSN

0363-6119

Authors

Cummings, Bethany P
Digitale, Erin K
Stanhope, Kimber L
et al.

Publication Date

2008-12-01

DOI

10.1152/ajpregu.90635.2008

Peer reviewed

Am J Physiol Regul Integr Comp Physiol 295: R1782–R1793, 2008.
First published October 1, 2008; doi:10.1152/ajpregu.90635.2008.

Development and characterization of a novel rat model of type 2 diabetes mellitus: the UC Davis type 2 diabetes mellitus UCD-T2DM rat

Bethany P. Cummings,[1,2] Erin K. Digitale,[2] Kimber L. Stanhope,[1,2] James L. Graham,[1,2] Denis G. Baskin,[3] Benjamin J. Reed,[4] Ian R. Sweet,[4] Steven C. Griffen,[5] and Peter J. Havel[1,2]

[1]*Department of Molecular Biosciences, School of Veterinary Medicine;* [2]*Department of Nutrition, University of California, Davis, California;* [3]*Research and Development Service, Department of Veterans Affairs Puget Sound Health Care System and Department of Medicine, Division of Metabolism, Endocrinology, and Nutrition;* [4]*Department of Medicine, University of Washington, Seattle, Washington; and* [5]*Department of Internal Medicine, University of California, Davis, Sacramento, California*

Submitted 27 July 2008; accepted in final form 26 September 2008

Cummings BP, Digitale EK, Stanhope KL, Graham JL, Baskin DG, Reed BJ, Sweet IR, Griffen SC, Havel PJ. Development and characterization of a novel rat model of type 2 diabetes mellitus: the UC Davis type 2 diabetes mellitus UCD-T2DM rat. *Am J Physiol Regul Integr Comp Physiol* 295: R1782–R1793, 2008. First published October 1, 2008; doi:10.1152/ajpregu.90635.2008.—The prevalence of type 2 diabetes (T2DM) is increasing, creating a need for T2DM animal models for the study of disease pathogenesis, prevention, and treatment. The purpose of this project was to develop a rat model of T2DM that more closely models the pathophysiology of T2DM in humans. The model was created by crossing obese Sprague-Dawley rats with insulin resistance resulting from polygenic adult-onset obesity with Zucker diabetic fatty-lean rats that have a defect in pancreatic β-cell function but normal leptin signaling. We have characterized the model with respect to diabetes incidence; age of onset; longitudinal measurements of glucose, insulin, and lipids; and glucose tolerance. Longitudinal fasting glucose and insulin data demonstrated progressive hyperglycemia (with fasting and fed glucose concentrations >250 and >450 mg/dl, respectively) after onset along with hyperinsulinemia resulting from insulin resistance at onset followed by a progressive decline in circulating insulin concentrations, indicative of β-cell decompensation. The incidence of diabetes in male and female rats was 92 and 43%, respectively, with an average age of onset of 6 mo in males and 9.5 mo in females. Results from intravenous glucose tolerance tests, pancreas immunohistochemistry, and islet insulin content further support a role for β-cell dysfunction in the pathophysiology of T2DM in this model. Diabetic animals also exhibit glycosuria, polyuria, and hyperphagia. Thus diabetes in the UC Davis-T2DM rat is more similar to clinical T2DM in humans than in other existing rat models and provides a useful model for future studies of the pathophysiology, treatment, and prevention of T2DM.

diabetic rodent model; hyperglycemia; insulin; β-cell

TYPE 2 DIABETES MELLITUS (T2DM) is a devastating metabolic disease presently affecting at least 16 million people in the United States alone (33, 49). The prevalence of T2DM is also increasing in children and adolescents (42). With the increasing incidence of T2DM, the identification of preventative measures has become crucial, necessitating the development of effective preclinical models for studying approaches for both diabetes prevention and treatment.

The most commonly used rodent models of T2DM include the Zucker diabetic fatty (ZDF) rat, the Otsuka Long Evans Tokushima fatty (OLETF) rat, and the *db/db* mouse, all of which exhibit obesity-associated insulin resistance and impaired β-cell function, resulting in diabetes (5, 25, 38). While these animal models have contributed substantially to understanding the pathophysiology and treatment of T2DM and its complications, the basic mechanisms underlying the pathogenesis of diabetes in these models do not correspond with what occurs in most human patients with T2DM. These differences in etiology are likely to hinder effective translational research.

Obesity and insulin resistance in most animal models of T2DM result from monogenic mutations that are rare in human and animal populations and present multiple problems in terms of applying these models to clinical T2DM. For example, mutations in the leptin receptor gene result in obesity and insulin resistance in both the ZDF rat and the *db/db* mouse (17, 37). Obesity in OLETF rats is thought to result in part from a single mutation in the gene encoding the CCK-A receptor (12, 13); however, these animals also exhibit other poorly characterized X-linked genetic defects (25). Relying on animal models with rare monogenic mutations for diabetes development is likely to produce confounding effects in studies utilizing these models. For example, leptin receptors expressed in pancreatic β-cells (27) have been implicated in the regulation of β-cell function (46, 47, 56). The absence of leptin signaling in the ZDF rat and the *db/db* mouse can therefore result in effects on β-cell function that are atypical of the human disease. In addition, leptin opposes insulin resistance, in part, via activation of AMP kinase causing a reduction in lipid deposition in insulin-sensitive tissues (20). Thus the lack of effective leptin signaling in ZDF rats and *db/db* mice promotes the development of diabetes involving mechanisms that do not commonly occur in clinical diabetes in humans. Furthermore, defective leptin signaling results in severe obesity and insulin resistance at a very early age. ZDF rats are obese at weaning (36) and hyperglycemic by 7–10 wk of age (37), whereas human obesity and insulin resistance resulting in T2DM are typically less severe and more often appear in adolescence and adulthood (18). This characteristic of early diabetes onset limits the use of currently available rodent models in diabetes prevention studies.

Leptin deficiency and leptin signaling defects also result in complete infertility in females (58); however, infertility is not

Address for reprint requests and other correspondence: P. J. Havel, Dept. of Molecular Biosciences, School of Veterinary Medicine, Univ. of California, Davis, One Shields Ave., Davis, CA 95616 (e-mail: pjhavel@ucdavis.edu).

The costs of publication of this article were defrayed in part by the payment of page charges. The article must therefore be hereby marked "*advertisement*" in accordance with 18 U.S.C. Section 1734 solely to indicate this fact.

a typical characteristic of diabetes in humans. This lack of fertility also makes the propagation of ZDF rats difficult, as only heterozygous animals can be bred. Finally, for reasons that are not well understood, female rodents are generally resistant to the development of diabetes (24) or become diabetic only when fed high-fat, high-sugar diets (34). In contrast, in many population groups, women develop diabetes more frequently than men (28). These shortcomings of currently available models highlight the need for new rodent models of T2DM.

Because the development of T2DM in humans requires both peripheral insulin resistance and inadequate β-cell compensation, we sought to develop a new rat model demonstrating polygenic adult-onset obesity and diabetes development in both sexes with preserved leptin signaling and fertility. We hypothesized that these characteristics would be present in offspring produced by crossing obese insulin-resistant Sprague-Dawley (OSD) rats with ZDF-lean rats. The breeding strategy was to cross these two lines of nondiabetic rats, each of which has only one of the primary defects associated with T2DM, and to then use selective breeding to enrich for diabetes in subsequent generations. One founder line consisted of OSD rats that exhibit polygenic, adult-onset obesity and insulin resistance on a standard laboratory rat chow diet but do not develop diabetes due to robust β-cell compensation (52). The second founder line, ZDF-lean rats, do not possess the leptin receptor mutation but have a defect in pancreatic β-cell insulin production (15) that results in diabetes only in the setting of insulin resistance. These studies demonstrate that this breeding strategy successfully produced diabetes in both male and female animals with animals exhibiting adult-onset obesity, insulin resistance, impaired glucose tolerance, and eventual β-cell decompensation. This model provides several advantages over currently available models including obesity of polygenic rather than monogenic origin, a later age of onset, preserved fertility, and development of diabetes in both sexes.

METHODS

Animals. Rats were housed and bred in the animal facility in the Department of Nutrition at the University of California, Davis, and maintained on a 12-h light-dark cycle. The experimental protocols were approved by the University of California Davis Institutional Animal Care and Use Committee.

Obese Sprague-Dawley (OSD) rats were originally obtained from Charles River Laboratories (Wilmington, MA). These animals gain weight more rapidly than Sprague-Dawley rats purchased from a different vendor, Harlan Laboratories (Indianapolis, IN; Ref. 51). The OSD rats exhibit adult-onset obesity and are hyperphagic and more metabolically efficient than normal weight animals (35, 39, 51). This obese phenotype appears polygenic in origin (31), with the OSD littermates exhibiting a wide continuum of body weights, rather than distinct "obese" and "lean" phenotypes as observed in monogenic models of obesity. Compared with lean Sprague-Dawley rats (LSD), OSD rats exhibit an early increase of visceral adipose mass and low circulating adiponectin concentrations (at 1 mo of age); increased fasting insulin concentrations and hepatic triglyceride (TG) deposition (at 3 mo); increased plasma nonesterified fatty acids and muscle TG content (at 6 mo); and progressive insulin resistance over their life span. However, even at 20 mo of age, they have only minimally elevated fasting glucose (112 mg/dl vs. 97 mg/dl in OSD and LSD rats, respectively; $P = 0.02$) and thus do not develop diabetes (52). In this regard, OSD rats are similar to most obese humans who develop insulin resistance but have robust β-cell function, which allows for sufficient compensatory insulin secretion and hyperinsulinemia without hyperglycemia.

ZDF-lean founder animals were purchased from Charles River Laboratories and genotyped via the tail-snip method to confirm that all founder animals were homozygous wild-type (+/+) at the leptin receptor locus (40). ZDF-lean rats have the autosomal recessive β-cell defect (15) but have functional leptin receptors and thus do not develop obesity or insulin resistance and are fertile. β-Cell function, although impaired, is sufficient to maintain normoglycemia in the absence of obesity-induced insulin resistance.

Breeding strategy. ZDF-lean male rats were mated with OSD females to produce the F1 generation, which was heterozygous for the autosomal recessive β-cell defect; thus animals did not develop diabetes. The heaviest F1 animals were bred to siblings to produce the F2 generation. Body weight and nonfasting blood glucose were monitored every 2 wk with a glucose meter (One-Touch Ultra; LifeScan, Milpitas, CA) in the F2 and subsequent generations. Diabetes onset was defined as a nonfasting blood glucose concentration >200 mg/dl obtained on two consecutive measurements, and the age of onset was defined as the age at which hyperglycemia was first detected. For F3 and subsequent generations, obese and hyperglycemic animals were bred to siblings with the goal of maintaining the obese phenotype and selecting for individuals homozygous for the autosomal recessive β-cell defect. Starting with the F7 generation, all animals were produced from matings in which both parents were either currently diabetic or subsequently developed diabetes, meaning that all animals are considered homozygous for the β-cell defect.

Characterization of diabetes incidence rates. Diabetes incidence and age of onset were systematically characterized in the F7 generation, with all animals in this generation undergoing body weight and nonfasted blood glucose monitoring until diabetes onset was reached. This was the first generation chosen to determine diabetes incidence since this was the first generation in which all animals were homozygous for the β-cell defect, and therefore, all animals in this generation and onward had the genetic propensity to develop diabetes. Animals were weaned at 21 days, housed in polycarbonate cages, and fed a standard commercial diet (no. 5008; Ralston Purina, Belmont, CA) and deionized water ad libitum.

Eighteen-month longitudinal study. Body weight, energy intake, and plasma lipids and hormones were determined before and after diabetes onset in a cohort of 16 male rats from the F9 and F10 generations. Rats were individually housed on hanging wire cages and provided ground chow (no. 5012; Ralston Purina; supplemented with safflower oil to 24% of energy as fat) in spill-resistant jars for accurate food intake measurements. Food intake and body weight were measured three times a week, and nonfasted blood glucose concentrations were monitored weekly at 1500. Diabetes onset was defined as described above. Fasted blood samples were collected once a month after an overnight (12 h) fast in EDTA-treated tubes and were analyzed for glucose, insulin, glucagon, free fatty acids (FFA), TG, leptin, adiponectin, and ghrelin.

Intravenous glucose tolerance testing. Glucose tolerance tests were performed on unanesthetized male F12 and F13 animals before onset (at 3 mo of age), 3 wk after diabetes onset, and 3 mo after diabetes onset. Animals were fasted overnight, and a 27-gauge butterfly catheter was placed in the saphenous vein for infusion of a bolus dose of 500 mg/kg body wt of a 50% dextrose solution. Blood samples were collected from the tail at 0, 2.5, 5, 10, 20, 30, 45, 60, 90, 120, and 180 min after glucose administration.

Islet immunohistochemistry. Pancreas samples were obtained from four groups of male rats: 4-mo-old LSD rats obtained from Harlan as a control; 4-mo-old nondiabetic University of California, Davis, type 2 diabetes mellitus (UCD-T2DM) rats; and UCD-T2DM rats 3 wk and 3 mo after diabetes onset. Briefly, pancreas samples were dissected under pentobarbital anesthesia and placed in 4% paraformaldehyde at 4°C and imbedded in paraffin. Sections (6-μM thick) were treated with 0.3% hydrogen peroxide for 30 min, followed by 5% normal goat

serum in PBS, and then immunostained following a standard protocol (57). Antibodies used were *1*) monoclonal anti-insulin (Sigma I-2018) at 6 μg/ml; and *2*) monoclonal anti-glucagon (Sigma G-2654) at 10 μg/ml, 4°C overnight. Detection of insulin and glucagon was by the ABC Elite kit (Vectastain PK-6100, Vector Laboratories) and diaminobenzidine-H_2O_2 (Vector SK-4100), and counterstained in hematoxylin. For controls, normal mouse IgG was substituted (Jackson ImmunoReserach 015-000-002) at 10 μg/ml. Controls showed no staining of islet cells. Original images of immunostained islets were captured as 16-bit RGB JPEG files. Each full original JPEG file was globally processed with the Auto Levels function of Adobe Photoshop to adjust color balance and contrast (no other manipulations were performed on the original image files).

Islet isolation, insulin content, and islet volume determination. Islets were isolated from age-matched (3 mo) pre- or postdiabetic male UCD-T2DM rats and LSD (Harlan, Livermore, CA) rats. Rats were anesthetized by intraperitoneal injection of sodium pentobarbital (150 mg/kg). Each isolation involved obtaining islets from three rat pancreases that were then pooled. Islets were prepared and purified as described previously (54) and then cultured for 18 h at 37°C in RPMI media 1640 supplemented with 10% heat-inactivated FBS (Invitrogen) before the experiments. Islets were examined under a TE-2000 Eclipse microscope (Nikon), and the number of islets less than or greater than 250 μm (as assessed using a calibrated reticle in the eyepiece) were counted and placed into separate dishes. Images of islets from each group were taken at ×4 magnification using a Nikon Coolpix camera mounted into the eyepiece of the microscope. Insulin content per islet was determined by placing islets from each group into wells of 24-well plates (5 islets into each of 3 wells) containing 0.2 ml of culture media, insulin was extracted by the addition of 1 ml of a mixture of ethanol and hydrochloric acid (2% v/v HCl to 95% ethanol), and the supernatant was collected after 60 min. Insulin was measured by ELISA (Mercodia, Uppsala, Sweden). Islet volume was estimated as follows. Images of at least 50 islets from each preparation were sized using ImageJ (National Institutes of Health, Bethesda, MD) by manually tracing around the perimeter of each islet using the virtual drawing tool, and the area within the region enclosed by the trace was calculated by the program. The diameter was calculated from the area as if the area was a circle according to the equation: $d = 2\times \text{ area}/\pi$. The volume of the idealized spherical islet was then calculated as $4/3\ \pi\ (d/2)^3$, and total islet volume for a preparation was the sum of the volumes of all the islets isolated.

Urinary glucose and albumin. Male rats from the F12 and F13 generations were studied to assess urinary glucose and albumin excretion. Twelve-hour urine samples were collected in sodium azide treated flasks and assayed for glucose and albumin. Urinary albumin excretion was measured using the Albumin Blue 580 fluorescence assay method described previously (26).

Visceral adiposity and liver and muscle TG content. Mesenteric adipose depots and liver and gastrocnemius muscle samples were obtained from four groups of 6-mo-old animals: LSD (Harlan) rats, OSD rats (Charles River), recently diabetic male F4 and F5, and weight-matched nondiabetic UCD-T2DM rats. The mesenteric adipose depot was dissected and weighed. Liver and muscle tissues were immediately placed in liquid nitrogen and stored at −80°C. Tissue TG was measured using the Folch method (9) for lipid extraction followed by spectrophotmetric measurement of TG content (Thermo Electron, Louisville, CO).

Assays. Plasma and urine glucose were measured using an enzymatic colorimetric assay for glucose (Thermo DMA). Insulin, leptin, glucagon, and adiponectin were measured with rodent/rat specific RIAs (Linco/Millipore, St. Charles, MO). Ghrelin was measured by RIA (rat-mouse ghrelin; Phoenix Pharmaceuticals, Burlingame, CA), and FFA and TG were measured with enzymatic colorimetric assays (NEFA Microtiter C kit, L-type TG H kit; Wako Chemicals, Richmond, VA).

Statistics and data analysis. Data are presented as means ± SE. Statistical analyses were performed using GraphPad Prism 4.00 for Windows (GraphPad Software, San Diego, CA). Longitudinal data were compared by one-way repeated measures ANOVA followed by post hoc analysis with Bonferroni's multiple comparison test. Incidence data divided into 2-mo body wt classes were analyzed by log-rank testing of Kaplan-Meier survival curves. Body weight and energy intake data in LSD compared with UCD-T2DM rats were compared by two-way repeated measures ANOVA followed by post hoc analysis with Bonferroni's multiple comparison test. Age of onset, mesenteric adipose weights, tissue TG and islet yield, size, and insulin content/islet volume results were analyzed by one-way ANOVA followed by post hoc analysis with Bonferroni's multiple comparison test. For the intravenous glucose tolerance test (IVGTT) data, the area under the curve (AUC) was calculated and compared by Student's *t*-test. Differences were considered significant at $P < 0.05$. Since the age of diabetes onset is not uniform, longitudinal data were analyzed by normalizing to the time of diabetes onset.

RESULTS

Both male and female UCD-T2DM rats develop diabetes. As previously discussed, the F7 generation is the generation for which a complete data set for age of onset and diabetes incidence is available for both male and female animals. Due to space limitations for housing animals, only male rats in subsequent generations have been monitored until diabetes onset. The incidence of diabetes in male and female rats in the F7 generation was 91.9% (102/111) and 42.6% (40/94) respectively, with the average age of onset being 183 ± 10 days in males and 286 ± 17 days in females (Table 1; $P < 0.0001$, males vs. females).

Kaplan-Meier survival analysis was performed to examine diabetes incidence in F7 female and F7 through F13 male rats. Division of animals into groups based on body weight at 2 mo of age demonstrates that early body weight greatly influences incidence and age of onset (Fig. 1, *A* and *B*). Male animals with a 2-mo body wt >400 g have an incidence of 99.1% with an average age of onset of 95 ± 5 days, whereas male rats weighing <350 g at 2 mo of age have an incidence of 86% and age of onset of 243 ± 13 days ($P < 0.0001$). The effect of

Table 1. *Incidence and age of onset in male and female UCD-T2DM rats*

Gender/Generation	Incidence, %	Age of Onset, day	*n*
Males			
F7	91.9	183±10	111
F7–F13, <350 g	86.0	243±13	93
F7–F13, 350–400 g	96.4	162±8*	112
F7–F13, >400 g	99.1	95±5*	107
Females			
F7	42.6	286±17†	94
F7, <240 g	21.1	375±19	57
F7, 240–270 g	59.1	326±22	22
F7, >270 g	100	179±17*	15

Values are means ± SE. UCD-T2DM, University of California, Davis, type 2 diabetes mellitus. *$P < 0.0001$, by Student's *t*-test, compared with lowest weight class. †$P < 0.0001$, by Student's *t*-test, compared with male F7 animals.

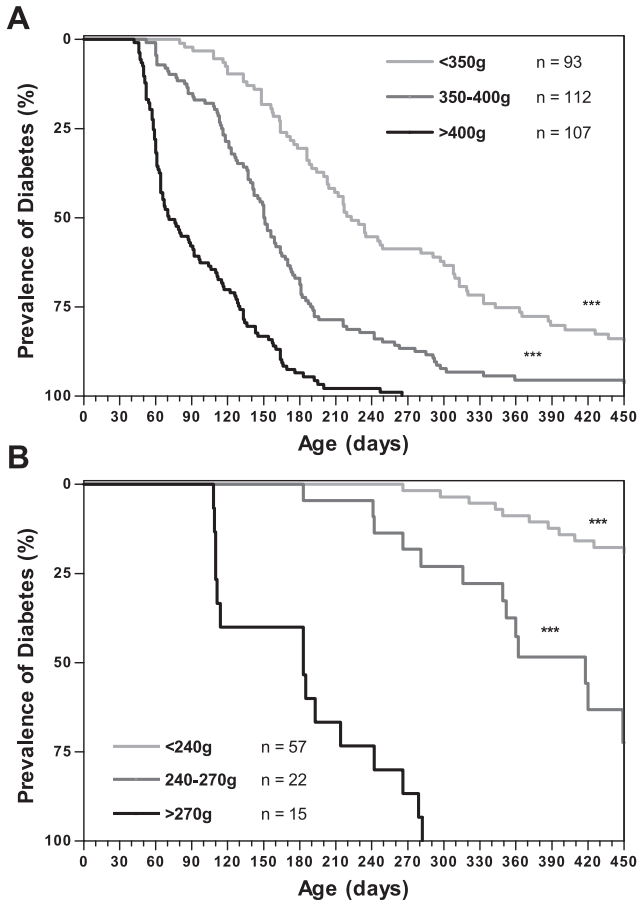

Fig. 1. Kaplan-Meier analysis of diabetes incidence in University of California, Davis, type 2 diabetes mellitus (UCD-T2DM) rats with animals categorized by body weight at 2 mo of age in male F7-F13 generations (*A*) and the female F7 generation (*B*). ***$P < 0.0001$ by log rank test compared with highest body weight class.

increased 2-mo body wt on incidence rate is even more pronounced in females. Female rats weighing <240 g at 2 mo have an incidence of 21% and an average age of onset of 375 ± 19 days, whereas 100% of females weighing >270 g at 2 mo of age develop diabetes with diabetes onset at 179 ± 17 days ($P < 0.0001$; Table 1).

Progressive hyperglycemia and inadequate β-cell compensation. The average age of onset in the cohort of male animals from the F9 and F10 generations that were monitored for 18 mo was 212 ± 16 days. Longitudinal measurements of plasma glucose and insulin concentrations centered at the time of diabetes onset demonstrate increasing insulin resistance before diabetes onset followed by inadequate pancreatic β-cell compensation at the time of onset and β-cell decompensation within 2–3 mo after onset (Fig. 2). Nonfasting hyperglycemia is present at onset (246 ± 12 mg/dl) and increases to 488 ± 18 mg/dl by 3 mo after onset ($P < 0.001$; Fig. 2). Fasting plasma glucose averaged 114 ± 2 mg/dl at onset and increased to 277 ± 22 mg/dl at 3 mo after onset ($P < 0.001$), suggesting that the hyperinsulinemia present at onset maintains lower glucose concentrations in the fasted state. Three months before onset fasting plasma insulin concentrations were 1.8 ± 0.3 ng/ml and increased to peak insulin levels of 3.4 ± 0.2 ng/ml at the time of diabetes onset ($P < 0.001$), corresponding with the increase in nonfasting glucose during the same period. Over the 3 mo after the development of hyperglycemia, there is a marked and progressive decline of fasting insulin levels (0.9 ± 0.2 ng/ml at 3 mo after onset; $P < 0.001$, compared with value at onset) despite the presence of pronounced fasting and nonfasting hyperglycemia.

Impaired glucose tolerance and loss of insulin secretion during IVGTT. Plasma glucose concentrations during IVGTT indicate impaired glucose clearance before diabetes onset compared with previous data from IVGTTs performed in LSD rats of similar age (8) and a marked deterioration of glucose homeostasis as diabetes progresses. At 3 wk after diabetes onset, the animals exhibit similar initial glucose excursions to prediabetic UCD-T2DM animals, but insulin excursions are significantly lower in recently diabetic compared with prediabetic animals (IVGTT insulin AUC: nondiabetic = 527 ± 58 and recently diabetic = 216 ± 44 ng/ml × 180 min; $P < 0.05$) in response to glucose administration. Three months after diabetes onset, there is a large increase in the glucose AUC, compared with prediabetic animals, (IVGTT glucose AUC: nondiabetic = 18,611 ± 2,191, recently diabetic = 17,706 ± 1,727, and diabetic for 3 mo = 30,528 ± 5,835 mg/dl × 180 min; $P < 0.001$) with plasma glucose concentrations remaining markedly elevated even 3 h after glucose administration. Similar to recently diabetic animals, circulating insulin does not increase in the 3-mo diabetic animals, remaining low despite marked hyperglycemia (Fig. 3, *A* and *B*). The insulin AUC is decreased by 88% compared with prediabetic animals (IVGTT insulin AUC: 3-mo diabetic = 64 ± 9 ng/ml × 180 min, $P < 0.005$).

Islet immunostaining and insulin secretion. Immunostaining for insulin and glucagon was performed on pancreas sections from selected animals from each group of animals that underwent IVGTT to examine islet morphology and to determine whether the failure to increase circulating insulin levels in diabetic animals in response to glucose administration was due to a reduction of insulin production. Figure 4 presents low magnification images of pancreas sections. These images suggest a progressive decrease of islet insulin staining with dia-

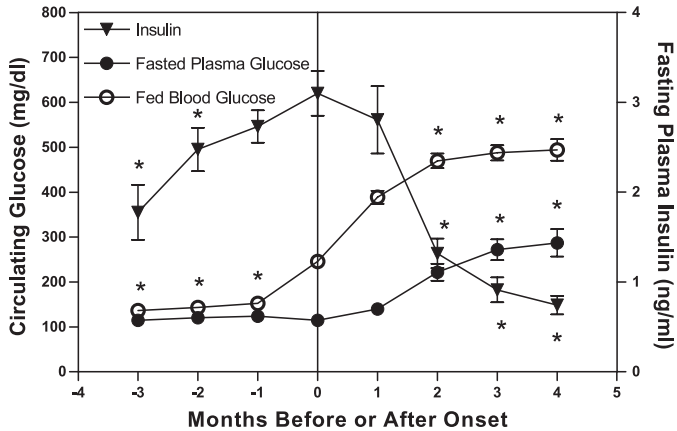

Fig. 2. Longitudinal nonfasted blood glucose and fasting plasma glucose and insulin concentrations before and after diabetes onset. Values are means ± SE. One-way repeated measures ANOVA, *P <0.001 by Bonferroni's posttest compared with value at onset ($n = 16$, $n = 14$ 4 mo after onset).

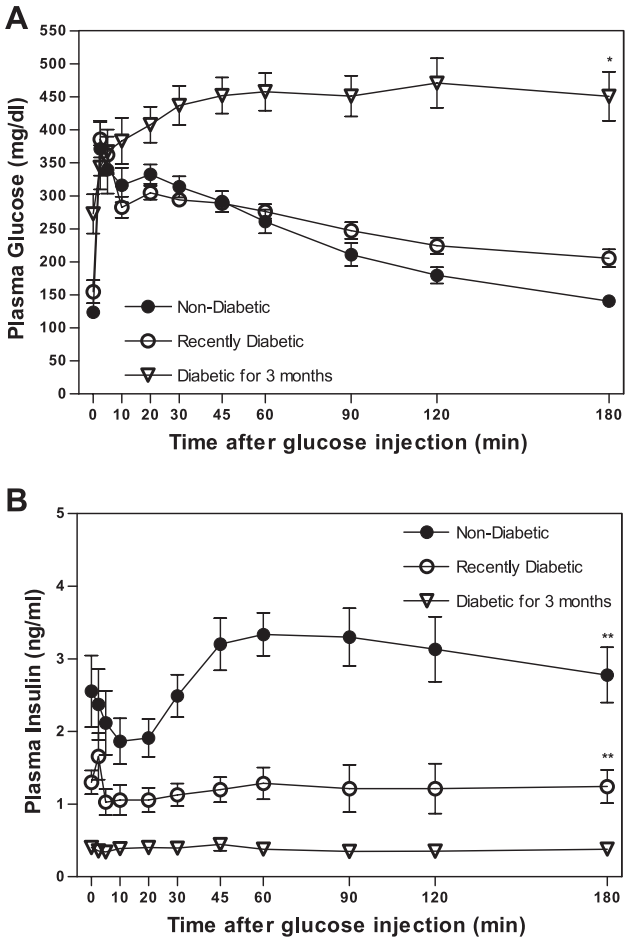

Fig. 3. Plasma glucose (*A*) and plasma insulin (*B*) excursions in response to intravenous glucose administration (500 mg/kg body wt and 50% dextrose solution) in nondiabetic, 3-wk diabetic, and 3-mo diabetic UCD-T2DM rats after an overnight fast. Values are means ± SE. Two-way repeated measures ANOVA, $*P < 0.01$ and $**P < 0.001$ by Bonferroni's posttest compared with the nondiabetic group ($n = 7$ per group).

betes progression. When compared with age-matched LSD controls (Harlan; Fig. 5, *A* and *B*), nondiabetic UCD-T2DM rat islets (Fig. 5, *B* and *C*) appear larger (likely hypertrophied). Immuostaining for insulin and glucagon suggests dispersion of α- and β-cells within these enlarged islets. Pancreas samples from 4-mo-old prediabetic UCD-T2DM animals appear to stain similarly for insulin and glucagon compared with animals with diabetes of 1-mo duration (data not shown). Figure 5, *E* and *F*, demonstrates the typical pathological islet morphology in animals with diabetes of 3-mo duration. These animals exhibit visibly reduced insulin and glucagon staining with widely dispersed α- and β-cells and marked disruptions in islet morphology.

To further study the characteristics of islets in the UCD-T2DM rats, islets were isolated from these rats before and after diabetes onset and their yield, size, volume and insulin content were determined. Animals were age and weight matched (11 wk and 440 ± 9 vs. 12 wk and 459 ± 13 g for the pre- and postdiabetic animals, respectively). Diabetic rats had been diabetic for ~3.5 wk. The control rats were LSD with an average age of 10 wk and an average body weight of 303 ± 8 g. Images of the isolated islets illustrate the increase in size and disruption of islet architecture in both pre- and postdiabetic rats (Fig. 6). To quantify the increase in size, islets were isolated from the three rat types, and the yields of islets that were below and above 250 μm, the maximal size measured in LSD rats, were determined (Fig. 7*A*). Approximately 55% of islets isolated from both pre- and postdiabetic UCD-T2DM rats were similar in size to those obtained from LSD rats. However, 45% of the islets were larger than the largest islets isolated from LSD rats. The total number of islets isolated from pre- and postdiabetic UCD-T2DM rats was >70% lower than LSD controls ($P < 0.001$). However, as an estimate of islet "mass," total islet volume was increased significantly in the UCD-T2DM rats relative to the LSD rats ($P < 0.05$; Fig. 7*B*). A similar trend was seen with islet area (data not shown). The actual areas and volumes may be an overestimate since islets that are not spherical will lay down in such a way as to expose the largest area. However, the method that measures islet "mass" increases in UCD-T2DM rats appears to be model independent. Importantly, islet yields were not reduced in diabetic rats compared with prediabetic rats. Notably, like islet volume, the insulin content in the prediabetic UCD-T2DM rats was more than fivefold higher than in islets from LSD rats ($P < 0.001$), and the insulin content per unit islet volume was greater in prediabetic compared with LSD rats ($P < 0.001$; Fig. 7*C*). Islet insulin content was dramatically decreased in the islets from diabetic UCD-T2DM rats ($P < 0.001$). Thus it appears that islet size and total volume are elevated in UCD-T2DM rat islets, but the transition from the prediabetic state to nonfasting hyperglycemia is associated with a marked decrease of insulin content, rather than a decrease of islet volume.

Other features of T2DM. UCD-T2DM rats exhibit adult-onset obesity and hyperphagia before developing diabetes, when compared with LSD rats, followed by a progressive increase in energy intake and slow loss of body weight after diabetes onset. Table 2 compares monthly body weight and energy intake by age in male UCD-T2DM rats with LSD rats. Female UCD-T2DM rats reach an adult body weight of 411 ± 7 g by 9 mo of age. Figure 8, *A* and *B*, shows body weight and energy intake before and after diabetes onset in male UCD-T2DM rats. One month before diabetes onset rats attain a body weight of 619 ± 16 g and consume 101 ± 4 kcal/day. After diabetes onset, there is a progressive increase in energy intake, with animals consuming 148 ± 8 kcal/day by 2 mo after onset ($P < 0.001$), indicative of hyperphagia observed in untreated diabetes after β-cell function has markedly declined. However, this increase in energy intake is not sufficient to compensate for the progressive impairment in glucose utilization, resulting in decreased body weight with animals losing 5 ± 1 and 11 ± 1% of peak body weight at 1 and 2 mo after onset, respectively ($n = 15$). Male rats studied during the F12 and F13 generations exhibited polyuria, glucosuria, and albuminuria after onset (Table 3).

Plasma lipids, visceral adiposity and tissue TG content. Before diabetes onset, circulating FFA concentrations remain stable at 0.76 ± 0.04 meq/l (value at 1 mo before onset). In contrast, plasma TGs progressively increase from 144 ± 22 mg/dl at 4 mo before onset to 193 ± 19 mg/dl at 1 mo before onset ($P < 0.01$; $n = 12$). Correspondingly, recently diabetic UCD-T2DM animals tend to have elevated mesenteric adipose weights and liver and muscle TG content compared with weight-matched nondiabetic UCD-T2DM animals. Liver and

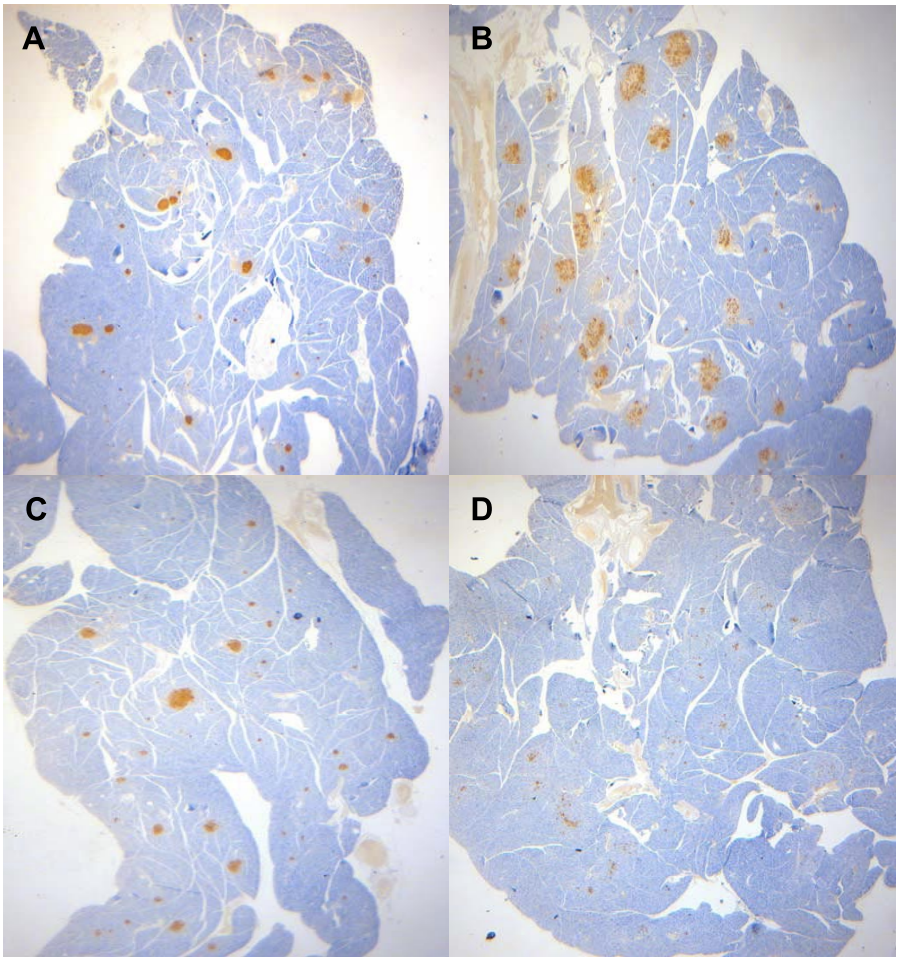

Fig. 4. Representative ×20 magnification images of anti-insulin immunohistochemical analysis of formalin-fixed pancreas sections from male lean Sprague-Dawley control rat (LSD) at 4 mo of age (*A*), nondiabetic UCD-T2DM rat at 4 mo of age (*B*), 1-mo diabetic UCD-T2DM rat at 3 mo of age (*C*), and 3-mo diabetic UCD-T2DM rat at 6 mo of age (*D*).

muscle TG contents are significantly elevated ($P < 0.01$) in recently diabetic UCD-T2DM animals when compared with age-matched LSD and OSD rats. Liver TG is also elevated in prediabetic UCD-T2DM rats compared with LSD controls ($P < 0.05$). Similar to OSD rats, mesenteric adipose weights are elevated in both prediabetic and diabetic UCD-T2DM rats compared with LSD controls ($P < 0.05$; Table 4). Circulating TGs decline from 223 ± 25 mg/dl at onset to 132 ± 18 mg/dl 2 mo after onset, suggesting a decrease in lipid availability in response to negative energy balance. Accordingly, plasma FFA increase to 0.89 ± 0.04 meq/l at 2 mo after onset ($P < 0.05$), which is likely the result of decreased inhibition of lipolysis by insulin.

Longitudinal hormone measurements. Fasting plasma leptin concentrations peaked at 11.6 ± 0.6 ng/ml at the time of diabetes onset and fell to 3.8 ± 0.6 ng/ml at 3 mo after onset ($P < 0.001$; Fig. 9*A*). Plasma adiponectin before diabetes onset was 5.2 ± 0.4 μg/ml (1 mo before onset) and decreased to 3.9 ± 0.3 μg/ml by 1 mo after onset ($P < 0.01$; Fig. 9*B*). Fasting plasma glucagon remained stable at 45 ± 2 pg/ml before onset (value taken 1 mo before onset) and increased to 58 ± 5 pg/ml by 4 mo after onset ($P < 0.05$; Fig. 9*C*). Circulating ghrelin concentrations were elevated by 4 mo after diabetes onset compared with values at onset (2,657 ± 382 vs. 1,913 ± 200 pg/ml; $P < 0.05$; Fig. 9*D*), corresponding with the time of peak hyperphagia.

DISCUSSION

By crossing an obese, insulin resistant Sprague-Dawley rat strain with ZDF-lean rats, we have generated a new rat model of T2DM with diabetes occurring in both sexes and with preserved leptin signaling and fertility. Preservation of leptin signaling was ensured by initial genotyping of ZDF-lean founder animals and was confirmed by demonstrating retained fertility in subsequent generations and by measurements of circulating leptin showing only modest increases of leptin compared with Zucker fatty (*fa/fa*) and ZDF rats. Fasting leptin concentrations peaked at 11.6 ± 0.6 ng/ml at the time of diabetes onset in the UCD-T2DM rats, whereas leptin concentrations in ZDF rats are reported to be >20 ng/ml (11) and >50 ng/ml in Zucker Fatty rats (29). Importantly, leptin concentrations in prediabetic animals are comparable with those in OSD rats from Charles River (29) and are appropriate for their degree of adiposity. By the F7 generation, all animals are considered to be homozygous for the β-cell defect since they are the offspring of diabetic parents. Thus all animals in this and subsequent generations have the genetic propensity to develop T2DM. Categorizing animals into groups based on body weight at 2 mo of age demonstrates that age of onset and incidence rate are highly influenced by early body weight. These data are consistent with clinical observations that obesity and insulin resistance lead to an earlier age of diabetes onset.

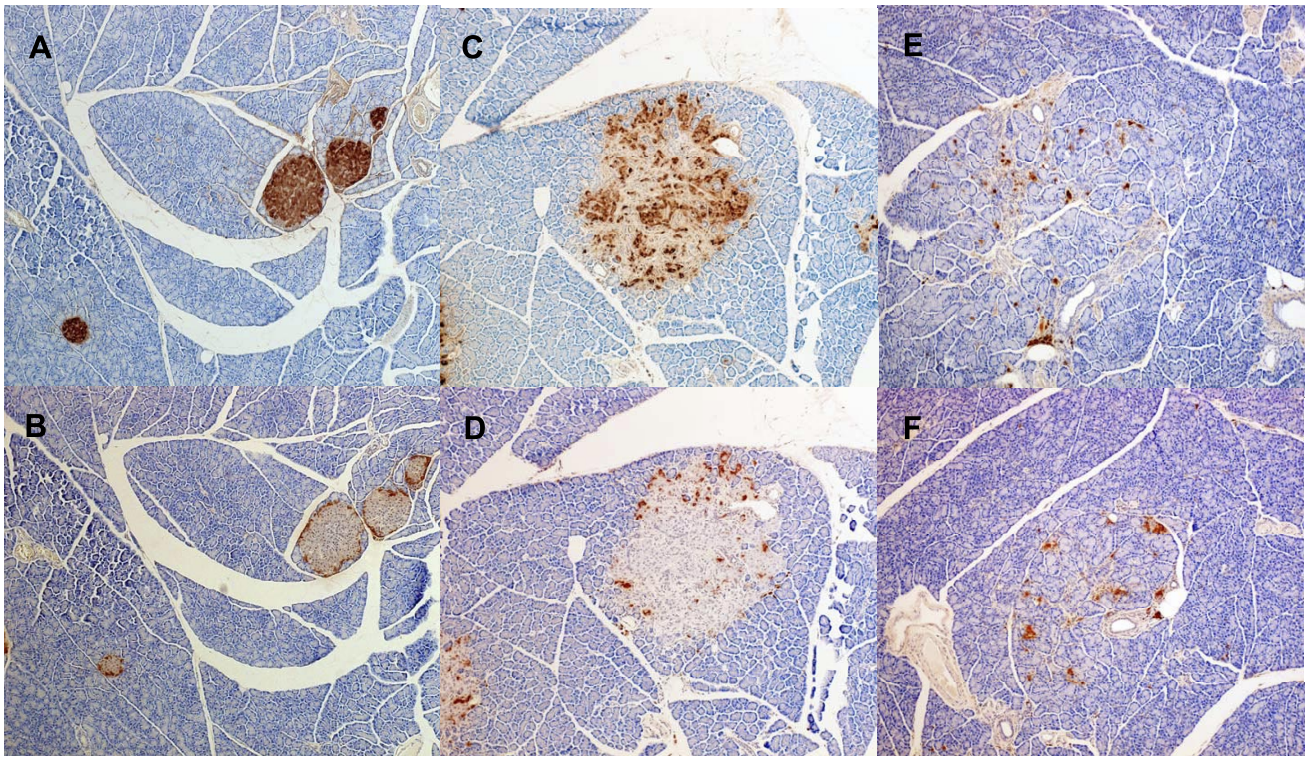

Fig. 5. Representative immunohistochemical analysis of pancreas sections from male LSD controls and UCD-T2DM rats at various stages of diabetes. All sections are at ×100 magnification. Anti-insulin immunohistochemistry staining for the following: *A*: LSD control at 4 mo of age; *C*: nondiabetic UCD-T2DM rat at 4 mo of age; and *E*: 3-mo diabetic UCD-T2DM rat at 6 mo of age. Anti-glucagon immunohistochemistry staining for the following: *B*: LSD control at 4 mo of age; *D*: nondiabetic UCD-T2DM rat at 4 mo of age; and *F*: 3-mo diabetic UCD-T2DM rat at 6 mo of age.

Multiple epidemiologic studies (2, 45) report an increased risk for T2DM and an earlier age of onset in people with an increased body mass index in youth and early adulthood. These results also provide a useful tool for planning studies in that animals can be selected based on 2-mo body wt to achieve a high or low incidence rate and an early or later age of diabetes onset.

The UCD-T2DM model provides several advantages over currently available diabetic animal models. First, the pathophysiolology of T2DM in these animals is more similar to that observed in clinical human and animal cases than other currently available models with monogenic mutations, such as those affecting leptin signaling that are extremely rare in humans and that also result in infertility and very early diabetes onset. In addition, elevated circulating TG, increased visceral adiposity, and ectopic lipid deposition are believed to play important roles in lipotoxicity and the pathogenesis of T2DM in humans (55); however, the lack of leptin signaling in many rodent models of the disease confounds results due to the absence of AMP kinase-mediated, anti-lipotoxic actions of leptin (20). The elevation of circulating TGs observed at onset in UCD-T2DM rats (223 ± 25 mg/dl) is modest compared with the extreme hypertriglyceridemia (plasma TG >1,000 mg/dl) observed in ZDF rats at diabetes onset (30). Thus the predia-

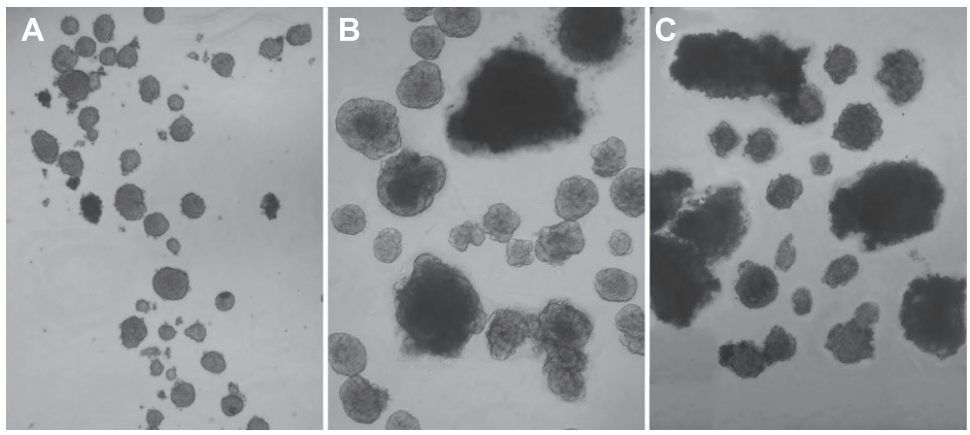

Fig. 6. Islet size and shape comparison of islets isolated from LSD controls rats (*A*), prediabetic (*B*), and diabetic UCD-T2DM (*C*) rats. All animals are at 2.5 to 3 mo of age and 3.5 wk of diabetes in the diabetic group.

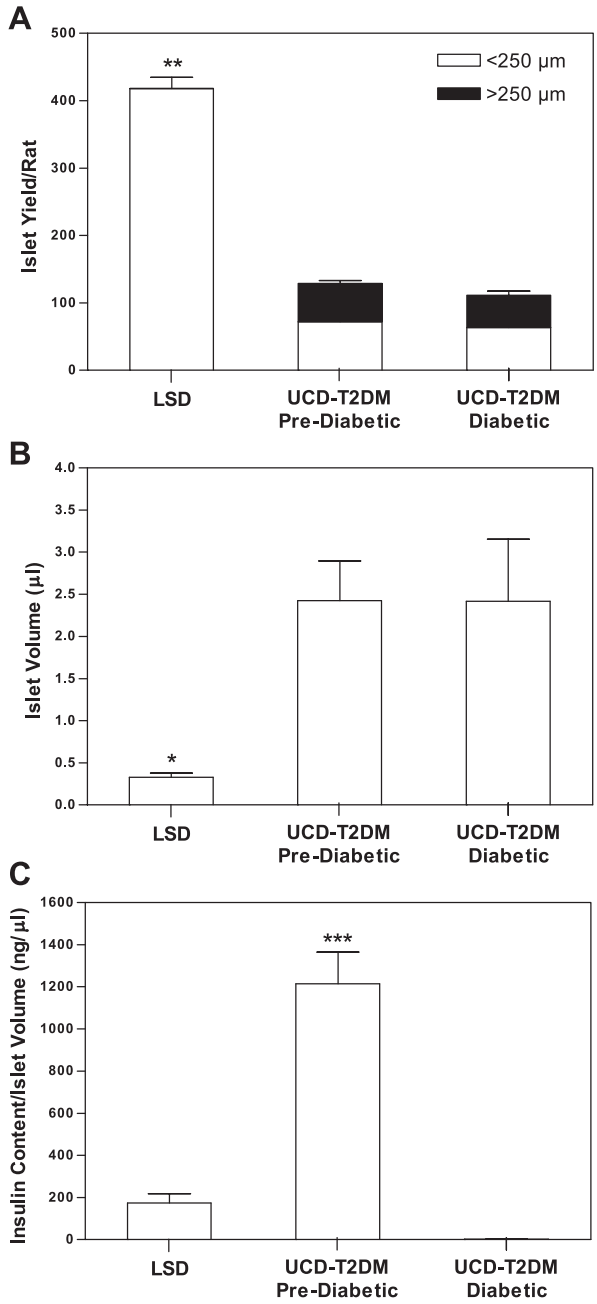

Fig. 7. Yield and size distribution of isolated islets (*A*; LSD: $n = 5$, prediabetic: $n = 5$, and diabetic: $n = 3$), islet volume (*B*: LSD: $n = 5$, prediabetic: $n = 5$, and diabetic: $n = 3$), and insulin content per islet volume (*C*: LSD: $n = 5$, prediabetic: $n = 5$, and diabetic: $n = 3$) in islets isolated from prediabetic and diabetic UCD-T2DM rats and LSD control rats at 2.5 to 3 mo of age and 3.5 wk of diabetes in the diabetic group. Values are means ± SE. One-way ANOVA, $*P < 0.05$, $**P < 0.001$ compared with prediabetic and diabetic UCD-T2DM rats and $***P < 0.001$ compared with LSD and diabetic UCD-T2DM rats by Bonferroni's posttest.

betic hypertriglyceridemia, increased visceral adiposity, and ectopic TG deposition present at onset in these animals appear more similar to what is observed clinically and support the lipotoxicity hypothesis that lipid dysregulation and deposition in muscle and liver contribute to insulin resistance in the pathogenesis of T2DM (10).

While there are some existing nonmonogenic models of diabetes such as the sand rat, which develops hyperglycemia

Table 2. *Monthly body weight and energy intake in lean Sprague-Dawley and UCD-T2DM male rats*

	LSD		UCD-T2DM	
Age, mo	Body wt, g	EI, kcal/day	Body wt, g	EI, kcal/day
1	97±2	48±1	118±3	50±4
2	260±4	72±2	365±9†	101±5*
3	323±6	68±2	510±13‡	99±3†
4	359±7	65±1	586±16‡	96±4†
5	388±7	65±3	618±16‡	92±4*
6	410±7	66±1	629±16‡	98±5*
7	431±9	68±1	627±18‡	104±7†
8	446±9	69±1	613±17‡	102±7†
9	454±8	64±4	595±17‡	111±7‡
10	476±8	65±2	566±19‡	123±8‡

Values are means ± SE. LSD: $n = 6$; and UCD-T2DM: $n = 16$. UCD-T2DM animals from F9 and F10 generations. Two-way repeated measures ANOVA: $*P < 0.05$, $†P < 0.001$, $‡P < 0.0001$, compared with lean Sprague-Dawley (LSD) rats by Bonferroni's posttest. EI, energy intake.

on a high-fat diet (48), and the high-fat diet-fed (HFD) streptozotocin-treated rat (50), these models require dietary and/or pharmaceutical manipulations whereas UCD-T2DM rats develop T2DM when fed a standard chow diet. The need for such additional treatments to produce diabetes in these models has

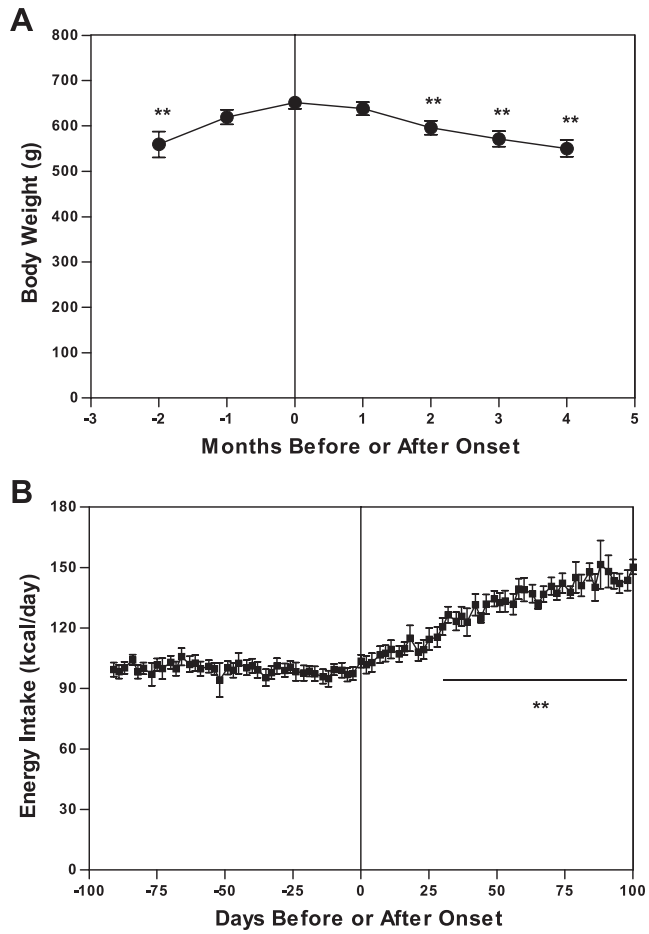

Fig. 8. Monthly body weight (*A*) and energy intake (*B*) before and after diabetes onset in UCD-T2DM rats. Values are means ± SE. One-way repeated measures ANOVA, $**P < 0.001$ by Bonferroni's posttest compared with value at onset ($n = 16$).

Table 3. *Urine volume, glucose, and UAE before and after diabetes onset in UCD-T2DM rats*

Months Before or After Onset	Urine Volume, ml/12 h	Urine Glucose, mg/dl	UAE, mg/day	*n*
−2	7±2	22±3	0.4±0.1	8
0	16±3	397±170†	0.7±0.1	8
3	31±8*	5,660±918†	3.2±1.0*	5

Values are means ± SE. UAE, urinary albumin excretion. One-way repeated-measures ANOVA: *$P < 0.01$, †$P < 0.001$, compared with 2 mo before onset by Bonferroni's posttest.

several disadvantages. For example, both of these animal models develop diabetes rapidly after the initiation of the diabetogenic treatment which makes these models difficult for use in the testing of preventative treatments. Furthermore, despite their polygenic obesity, these animal models still present etiologic disparities such as the need for pharmaceutically induced β-cell destruction in the HFD streptozotocin-treated rat and the extreme diet sensitivity expressed in the sand rat, with younger animals developing hyperglycemia within 14 days after initiation of a high-energy diet (23).

Inadequate insulin secretion to compensate for insulin resistance followed by eventual β-cell decompensation is a key component of the pathogenesis of clinical T2DM (22) and is clearly demonstrated in this model through longitudinal measurements of glucose and insulin and through results from IVGTTs, islet immunohistochemistry, and islet insulin content. These results demonstrate a progressive loss of the ability to maintain insulin production and glucose homeostasis, with corresponding degenerative changes in islet morphology, and decreased insulin staining and insulin content. The timing of changes of insulin concentrations relative to diabetes onset presented in Fig. 2 is similar to that seen in humans: insulin levels rise significantly before diabetes onset, peak around the time of onset, and decline as hyperglycemia becomes more pronounced (21). Insulin immunostaining and measurement of insulin content in isolated islets confirm the reduction in insulin content with the progression of diabetes in these animals, corresponding with what would be expected from the autosomal recessive insulin promoter defect that is characteristic of this model (15). Previous studies (32, 41) on islet histology of lean ZDF rats do not demonstrate severe disruptions in islet morphology or β-cell mass. Our results thus confirm the hypothesis that the pancreatic defect present in the ZDF lean rat becomes pronounced only when the islets are challenged by the presence of obesity-induced insulin resistance. Thus the β-cells of UCD-T2DM rats fail to adequately compensate for obesity-induced insulin resistance. Furthermore, similar to clinical T2DM, glucagon levels are elevated starting 4 mo after onset, supporting a role for α-cell dysregulation in the maintenance and progression of T2DM (7). Thus this model may provide insight into the relative contributions of insulin resistance and islet dysfunction in T2DM pathogenesis. Further studies on what causes the observed β-cell hypertrophy and disruptions of islet morphology are needed.

There are a number of important and unique features that support the utility of the UCD-T2DM rat as a model of T2DM. With the preservation of leptin signaling, the animals remain fertile. Preservation of fertility makes this model highly efficient for T2DM studies in that all animals have the potential to develop diabetes and all animals can be used for breeding. The delayed onset of diabetes observed in UCD-T2DM rats allows for testing of therapies aimed at diabetes prevention. The UCD-T2DM rat manifests diabetes in both males and females, providing a much needed model for examining gender-specific characteristics of diabetes development. Specifically, female UCD-T2DM rats demonstrate polygenic adult-onset obesity, hyperglycemia, and albuminauria (data not shown). While the present studies mainly focused on characterizing the males, future studies will be carried out detailing the diabetic pathology present in females. In particular, successful pregnancies observed in females that developed diabetes while pregnant suggest that UCD-T2DM rats may be useful as a model for gestational diabetes, a disease for which a well-described rodent model is lacking (3).

In addition to its utility as a model of diabetes etiology, these animals appear to develop diabetic complications such as diabetic nephropathy and lipid dysregulation. UCD-T2DM rats demonstrate a 20% elevation in FFAs after onset, similar to what is observed in clinical T2DM (4) and have moderately elevated plasma TG concentrations before diabetes onset compared with LSD rats. Interestingly, a similar moderate (~38%) elevation of plasma TG levels has been observed in measurements made at 18, 12, and 6 mo before the diagnosis of diabetes in 86 human subjects who developed type 2 diabetes compared with 860 subjects who did not develop diabetes in the West of Scotland Coronary Prevention Study (44). UCD-T2DM rats exhibit diabetic renal complications as evidenced by markedly elevated urinary albumin excretion. These results suggest that the UCD-T2DM rat may serve as a useful model for diabetic nephropathy.

Finally, the metabolic abnormalities present in UCD-T2DM rats will provide productive grounds for future studies investigating the role of other hormones in the pathogenesis of T2DM. For example, it is an ideal model to study the role of and mechanisms by which decreased circulating adiponectin concentrations are involved in the progression of T2DM. Adiponectin is secreted by adipocytes in inverse proportion to visceral adiposity and has insulin-sensitizing and anti-inflammatory effects (16, 19, 53). Obese humans with T2DM have lower circulating adiponectin concentrations than nondiabetic individuals (16). Similarly, circulating adiponectin concentrations in male UCD-T2DM animals were 25% lower after diabetes onset. This model may also provide insight into the role of ghrelin in T2DM progression. The observed increase

Table 4. *Visceral adipose weight and tissue triglyceride content in LSD, OSD, and nondiabetic and recently diabetic UCD-T2DM rats*

	Mesenteric	μM TG/g Tissue	
	Adipose Weight, g	Gastrocnemius	Liver
LSD	2.5±0.1	1.7±0.1	6.1±0.4
OSD	9.5±1.8‡	4.4±0.8	16.0±3.2
Nondiabetic	7.8±0.7†	10.3±1.8	20.1±5.1*
Diabetic	9.4±0.9‡	15.3±3.5†	32.4±3.4†

Values are means ± SE. (LSD: $n = 6$; obese Sprague Dawley (OSD): $n = 6$; nondiabetic: $n = 3$; and diabetic: $n = 6$]. One-way ANOVA: *$P < 0.05$, ‡$P < 0.001$, compared with LSD animals by Bonferroni's posttest. One-way ANOVA: †$P < 0.01$, compared with LSD and animals by Bonferroni's posttest. TG, triglyceride.

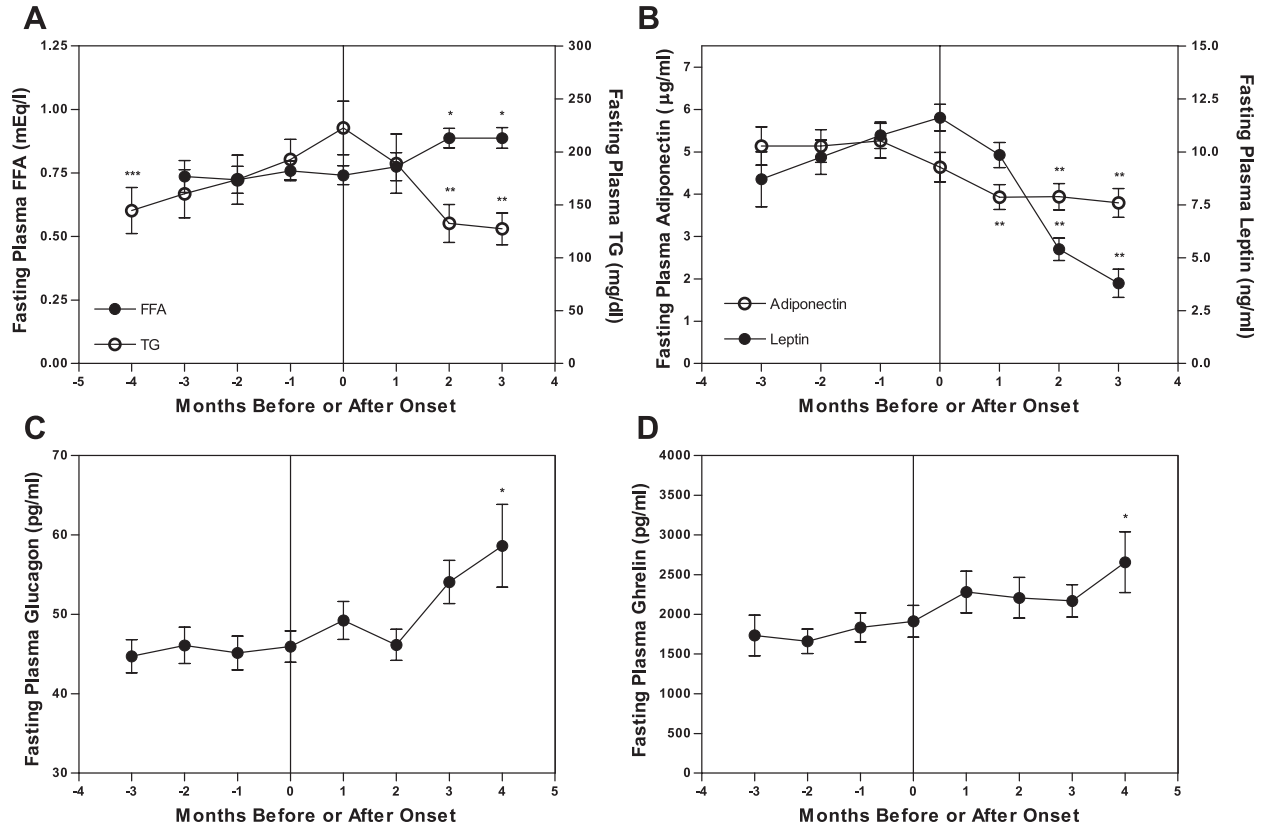

Fig. 9. *A*: longitudinal fasting plasma triglyceride (TG) and free fatty acids (FFA). TG: $n = 12$ at 4 mo before onset, $n = 16$ at all other time points; and FFA: $n = 12$ at 2 and 3 mo before onset, $n = 16$ at all other time points. *B*: longitudinal fasting plasma adiponectin and leptin. Adiponectin: $n = 16$ at all time points; and leptin: $n = 13$ at 3 mo before onset, $n = 16$ at all other time points. *C*: longitudinal fasting plasma glucagon: $n = 13$ at 4 mo after onset, $n = 16$ at all other time points. *D*: longitudinal fasting plasma ghrelin: $n = 12$. Values are means ± SE. One-way repeated measures ANOVA;, $*P < 0.05$, $** P < 0.001$ compared with value at onset; $***P < 0.05$ compared with value 1 mo before onset by Bonferroni's posttest.

of circulating ghrelin after diabetes onset may appear to contradict reports showing ghrelin to be lower in T2DM; however, these studies were conducted in subjects with treated T2DM and who are obese or overweight (43). Furthermore, ghrelin has been shown to be decreased by increased circulating levels of insulin (1, 14). This would suggest that the loss in body weight and insulin production observed after 4 mo of diabetes in this animal model may be involved in the increase of ghrelin. Given that ghrelin has been shown to inhibit insulin secretion (6), the increase of ghrelin after diabetes onset suggests a potential for ghrelin in diabetes progression.

Perspectives and Significance

In summary, the UCD-T2DM rat model exhibits a T2DM etiology more similar to clinical T2DM in humans than other rodent models such as the ZDF rat. These similarities include obesity and insulin resistance of polygenic origin, later ages of diabetes onset, development of diabetes in both male and female animals that occurs on a standard rodent chow diet, and importantly preserved fertility in both sexes (Table 5). Characterization of the model indicates that the UCD-T2DM rat will be a useful tool for investigating the pathophysiology, prevention, and treatment of T2DM.

Table 5. *Comparison of the UCD-T2DM rat with human T2DM and the ZDF rat model*

Characteristic	Human T2DM	UCD-T2DM Rat	ZDF Rat
Origin of obesity	Polygenic	Polygenic	Monogenic leptin receptor mutation
Inherited β-cell defect	Likely	Yes	Yes
Age of T2DM onset	Adolescent to adult	Males: 183±10 days; females: 286±17 days	Males: 60–90 days
Gender-specific onset	No	Female onset approximately 3 mo after males	Females develop diabetes only on a high-fat, high-sugar diet
Fertility	Preserved	Preserved	Infertile
Plasma TG elevation	Usually moderate	Moderate	Severe
Liver and muscle TG accumulation	Yes	Yes	Yes

ZDF, Zucker diabetic fatty.

ACKNOWLEDGMENTS

Islet isolation and assessment of islets was done by the Cellular and Molecular Imaging and Islet Cell and Functional Analysis Cores, University of Washington Diabetes Endocrinology Research Center.

We thank Joyce Murphy for excellent technical support with pancreas immunohistochemistry, Kimberley Nguyen for help with measurements of renal function, and Hong-Duc Ta for extensive help with animal care and monitoring.

GRANTS

Immunohistochemistry data are the result of work supported by facilities at the Veterans Affairs Puget Sound Health Care System (Seattle, WA). Dr. Baskin is Senior Research Career Scientist, Research and Development Service, Department of Veterans Affairs Puget Sound Health Care System. This research was also supported in part by the National Center for Complementary and Alternative Medicine Grant AT-002993 (to P. J. Havel) and National Institute of Diabetes and Digestive and Kidney Diseases DK-002619 and DK-060662 (both to S. C. Griffen). Dr. Havel's laboratory also receives support from National Heart, Lung, and Blood Institute Grants R01-HL-075675 and R01-HL-09333; National Center for Complementary and Alternative Medicine Grants AT-002599, AT-003545, and AT-003645; and the American Diabetes Association. Immunohistochemistry and islet analysis work were supported by National Institute of Diabetes and Digestive and Kidney Diseases Grant P30-DK-17047 through the Cellular and Molecular Imaging Core of the University of Washington Diabetes Endocrinology Research Center. Islet isolation work was supported by Merck Investigator-Initiated Studies Program (Study #33171).

REFERENCES

1. **Anderwald C, Brabant G, Bernroider E, Horn R, Brehm A, Waldhausl W, Roden M.** Insulin-dependent modulation of plasma ghrelin and leptin concentrations is less pronounced in type 2 diabetic patients. *Diabetes* 52: 1792–1798, 2003.
2. **Bhargava SK, Sachdev HS, Fall CH, Osmond C, Lakshmy R, Barker DJ, Biswas SK, Ramji S, Prabhakaran D, Reddy KS.** Relation of serial changes in childhood body-mass index to impaired glucose tolerance in young adulthood. *N Engl J Med* 350: 865–875, 2004.
3. **Caluwaerts S, Holemans K, van Bree R, Verhaeqhe J, Van Assche F.** Is low-dose streptozotocin in rats an adequate model for gestational diabetes? *J Soc Gynecol Investig* 10: 216–221, 2003.
4. **Carmena R.** Type 2 diabetes, dyslipidemia, and vascular risk: rationale and evidence for correcting the lipid imbalance. *Am Heart J* 150: 859–870, 2005.
5. **Chang AY.** Spontaneous diabetes in animals. *Gen Pharmac* 9: 447–450, 1978.
6. **Dezaki K, Kakei M, Yada T.** Ghrelin uses Galphai2 and activates voltage-dependent K+ channels to attenuate glucose-induced Ca2+ signaling and insulin release in islet beta-cells: novel signal transduction of ghrelin. *Diabetes* 56: 2319–2327, 2007.
7. **Dunning BE, Gerich JE.** The role of alpha-cell dysregulation in fasting and postprandial hyperglycemia in type 2 diabetes and therapeutic implications. *Endocr Rev* 28: 253–283, 2007.
8. **Ferrari B, Arnold M, Carr RD, Langhans W, Pacini G, Bodvarsdottir TB, Gram DX.** Subdiaphragmatic vagal deafferentation affects body weight gain and glucose metabolism in obese male Zucker (fa/fa) rats. *Am J Physiol Regul Integr Comp Physiol* 289: R1027–R1034, 2005.
9. **Folch J, Lees M, Sloane G, Stanley H.** A simple method for the isolation and purification of total lipides from animal tissues. *J Biol Chem* 226: 497–509, 1957.
10. **Frayn KN, Arner P, Yki-Jarvinen H.** Fatty acid metabolism in adipose tissue, muscle and liver in health and disease. *Essays Biochem* 42: 89–103, 2006.
11. **Fu W, Haynes T, Kohli R, Hu J, Shi W, Spencer T, Carroll R, Meininger C, Wu G.** Dietary L-arginine supplementation reduces fat mass in Zucker diabetic fatty rats. *J Nutr* 134: 714–721, 2005.
12. **Funakoshi A, Miyasaka K, Kanai S, Masuda M, Yasunami Y, Nagai T, Ikeda S, Jimi A, Kawanami T, Kono A.** Pancreatic endocrine dysfunction in rats not expressing the cholecystokinin-A receptor. *Pancreas* 12: 230–236, 1996.
13. **Funakoshi A, Miyasaka K, Shinozaki H, Masuda M, Kawanami T, Takata Y, Kono A.** An animal model of congenital defect of gene expression of cholecystokinin (CCK)-A receptor. *Biochem Biophys Res Commun* 210: 787–796, 1995.
14. **Griffen SC, Oostema K, Stanhope KL, Graham J, Styne DM, Glaser N, Cummings DE, Connors MH, Havel PJ.** Administration of Lispro insulin with meals improves glycemic control, increases circulating leptin, and suppresses ghrelin, compared with regular/NPH insulin in female patients with type 1 diabetes. *J Clin Endocrinol Metab* 91: 485–491, 2006.
15. **Griffen SC, Wang J, German MS.** A genetic defect in beta-cell gene expression segregates independently from the fa locus in the ZDF rat. *Diabetes* 50: 63–68, 2001.
16. **Havel PJ.** Update on adipocyte hormones: regulation of energy balance and carbohydrate/lipid metabolism. *Diabetes* 53: S143–S148, 2004.
17. **Herberg L, Leiter EH.** Obesity/diabetes in mice with mutations in the leptin or leptin receptor genes. In: *Animal Models of Diabetes: A Primer*, edited by Sima AAF and Shafrir E. Amsterdam, The Netherlands: Harwood Academic, 2001, p. 63–107.
18. **Hogikyan RV, Halter JB.** Aging and diabetes. In: *Diabete Mellitus* (5th ed.), edited by Porte D and Sherwin RS. Stamford, CT: Appleton and Lange, 1997, p. 565–580.
19. **Kadowaki T, Yamauchi T.** Adiponectin and adiponectin receptors. *Endocr Rev* 26: 439–451, 2005.
20. **Kahn BB, Alquier T, Carling D, Hardie DG.** AMP-activated protein kinase: ancient energy gauge provides clues to modern understanding of metabolism. *Cell Metab* 1: 15–25, 2005.
21. **Kahn SE, Porte D.** The pathophysiology of type II (non-insulin dependent) diabetes mellitus: implications for treatment. In: *Diabetes Mellitus* (5th ed.), edited by Porte D and Sherwin RS. Stamford, CT: Appleton and Lange, 1997, p. 487–512.
22. **Kahn SE, Prigeon RL, Schwartz RS, Fujimoto WY, Knopp RH, Brunzell JD, Porte D.** Obesity, body fat distribution, insulin sensitivity and islet beta-cell function as explanations for metabolic diversity. *J Nutr* 131: 354S–360S, 2001.
23. **Kalman R, Ziv E, Shafrir E, Bar-On H, Perez R.** Psammomys obesus and the albino rat–two different models of nutritional insulin resistance, representing two different types of human populations. *Lab Anim* 35: 346–352, 2001.
24. **Kawano K, Hirashima T, Mori S, Man ZW, Natori T.** The OLETF rat. In: *Animal Models of Diabetes: A Primer*, edited by Sima AAF and Shafrir E. Amsterdam, The Netherlands: Harwood Academic, 2001, p. 213–225.
25. **Kawano K, Hirashima T, Mori S, Natori T.** OLETF (Otsuka Long-Evans Tokushima fatty) rat: a new NIDDM rat strain. *Diabetes Res Clin Pract* 24 *Suppl*: S317–S320, 1994.
26. **Kessler MA, Meinitzer A, Petek W, Wolfbeis OS.** Microalbuminuria and borderline-increased albumin excretion determined with a centrifugal analyzer and the Albumin Blue 580 fluorescence assay. *Clin Chem* 43: 996–1002, 1997.
27. **Kieffer TJ, Heller RS, Habener JF.** Leptin receptors expressed on pancreatic beta-cells. *Biochem Biophys Res Commun* 224: 522–527, 1996.
28. **King H, Aubert RE, Herman WH.** Global burden of diabetes, 1995–2025: prevalence, numerical estimates, and projections. *Diabetes Care* 21: 1414–1431, 1998.
29. **Landt M, Gingerich R, Havel PJ, Mueller W, Schoner B, Hale J, Heiman M.** Radioimmunoassay of rat leptin: sexual dimorphism reversed from humans. *Clin Chem* 44: 565–570, 1998.
30. **Lee Y, Hirose H, Ohneda M, Johnson JH, McGarry JD, Unger RH.** Beta-cell lipotoxicity in the pathogenesis of non-insulin-dependent diabetes mellitus of obese rats: impairment in adipocyte-beta-cell relationships. *Proc Natl Acad Sci USA* 91: 10878–10882, 1994.
31. **Levin BE, Dunn-Meynell AA, Balkan B, Keesey RE.** Selective breeding for diet-induced obesity and resistance in Sprague-Dawley rats. *Am J Physiol Regul Integr Comp Physiol* 273: R725–R730, 1997.
32. **Li X, Zhang L, Meshinchi S, Dias-Leme C, Raffin D, Johnson JD, Treutelaar MK, Burant CF.** Islet microvasculature in islet hyperplasia and failure in a model of type 2 diabetes. *Diabetes* 55: 2965–2973, 2006.
33. **Meetoo D, McGovern P, Safadi R.** An epidemiological overview of diabetes across the world. *Br J Nurs* 16: 1002–1007, 2007.
34. **Noguchi T, Tanaka T.** Insulin resistance in obesity and its molecular control. *Obes Res* 3: 195s–198s, 1995.
35. **Nohynek GJ, Longeart L, Geffray B, Provost JP, Lodola A.** Fat, frail and dying young: survival, body weight and pathology of the Charles River Sprague-Dawley-derived rat prior to and since the introduction of the VAFR variant in 1988. *Hum Exp Toxicol* 12: 87–98, 1993.
36. **Park ES, Seong JK, Yi SJ, Kim JS, Lee HS, Lee IS, Yoon YS.** Changes in orexin-A and neuropeptide Y expression in the hypothal-

amus of obese and lean Zucker diabetic fatty rats. *J Vet Med Sci* 67: 639–646, 2005.
37. **Peterson RG.** The Zucker Diabetic Fatty (ZDF) Rat. In: *Animal Models of Diabetes: A Primer*, edited by Sima AAF and Shafrir E. Amsterdam, The Netherlands: Harwood Academic, 2001, p. 109–128.
38. **Peterson RG, Shaw WN, Neel MA, Little LA, Eichberg J.** Zucker diabetic fatty rat as a model for non-insulin-dependent diabetes mellitus. *ILAR News* 32: 16–19, 1990.
39. **Pettersen JC, Morrissey RL, Saunders DR, Pavkov KL, Luempert LG, 3rd Turnier JC, Matheson DW, Schwartz DR.** A 2-year comparison study of Crl:CD BR and Hsd:Sprague-Dawley SD rats. *Fundam Appl Toxicol* 33: 196–211, 1996.
40. **Phillips MS, Liu Q, Hammond HA, Dugan V, Hey PJ, Caskey CJ, Hess JF.** Leptin receptor missense mutation in the fatty Zucker rat. *Nat Genet* 13: 18–19, 1996.
41. **Pick A, Clark J, Kubstrup C, Levisetti M, Pugh W, Bonner-Weir S, Polonsky KS.** Role of apoptosis in failure of beta-cell mass compensation for insulin resistance and beta-cell defects in the male Zucker diabetic fatty rat. *Diabetes* 47: 358–364, 1998.
42. **Pihoker C, Scott CR, Lensing SY, Cradock MM, Smith J.** Non-insulin dependent diabetes mellitus in African-American youths of Arkansas. *Clin Pediatr* 37: 97–102, 1998.
43. **Poykko SM, Kellokoski E, Horkko S, Kauma H, Kesaniemi YA, Ukkola O.** Low plasma ghrelin is associated with insulin resistance, hypertension, and the prevalence of type 2 diabetes. *Diabetes* 52: 2546–2553, 2003.
44. **Sattar N, McConnachie A, Ford I, Gaw A, Cleland SJ, Forouhi NG, McFarlane P, Shepherd J, Cobbe S, Packard C.** Serial metabolic measurements and conversion to type 2 diabetes in the west of Scotland coronary prevention study: specific elevations in alanine aminotransferase and triglycerides suggest hepatic fat accumulation as a potential contributing factor. *Diabetes* 56: 984–991, 2007.
45. **Schienkiewitz A, Schulze MB, Hoffmann K, Kroke A, Boeing H.** Body mass index history and risk of type 2 diabetes: results from the European Prospective Investigation into Cancer and Nutrition (EPIC)-Potsdam Study. *Am J Clin Nutr* 84: 427–433, 2006.
46. **Seufert J, Kieffer TJ, Habener JF.** Leptin inhibits insulin gene transcription and reverses hyperinsulinemia in leptin-deficient ob/ob mice. *Proc Natl Acad Sci USA* 96: 674–679, 1999.
47. **Seufert J, Kieffer TJ, Leech CA, Holz GG, Moritz W, Ricordi C, Habener JF.** Leptin suppression of insulin secretion and gene expression in human pancreatic islets: implications for the development of adipogenic diabetes mellitus. *J Clin Endocrinol Metab* 84: 670–676, 1999.
48. **Shafrir E, Ziv E, Kalman R.** Nutritionally induced diabetes in desert rodents as models of type 2 diabetes: Acomys cahirinus (spiny mice) and Psammomys obesus (desert gerbil). *ILAR J* 47: 212–224, 2006.
49. **Siegel K, Narayan KM.** The Unite for Diabetes campaign: overcoming constraints to find a global policy solution. *Global Health* 4: 3, 2008.
50. **Srinivasan K, Viswanad B, Asrat L, Kaul CL, Ramarao P.** Combination of high-fat diet-fed and low-dose streptozotocin-treated rat: a model for type 2 diabetes and pharmacological screening. *Pharmacol Res* 52: 313–320, 2005.
51. **Stanhope KL, Kras KM, Moreno-Aliaga MJ, Havel PJ.** A comparison of adipocyte size and metabolism in Charles River and Harlan Sprague Dawley rats (Abstract). *Obes Res* 8: 66S, 2000.
52. **Stanhope KL, Sinha M, Graham J, Havel PJ.** Low circulating adiponectin levels and reduced adipocyte adiponectin production in obese, insulin-resistant Sprague-Dawley rats (Abstract). *Diabetes* 52: A404, 2002.
53. **Swarbrick MM, Havel PJ.** Physiological, pharmacological, and nutritional regulation of circulating adiponectin concentrations in humans. *Metab Syndr Relat Disord* 6: 87–102, 2008.
54. **Sweet IR, Cook DL, DeJulio E, Wallen AR, Khalil G, Callis J, Reems J.** Regulation of ATP/ADP in pancreatic islets. *Diabetes* 53: 401–409, 2004.
55. **Unger RH.** Longevity, lipotoxicity and leptin: the adipocyte defense against feasting and famine. *Biochimie* 87: 57–64, 2005.
56. **Wang MY, Koyama K, Shimabukuro M, Mangelsdorf D, Newgard CB, Unger RH.** Overexpression of leptin receptors in pancreatic islets of Zucker diabetic fatty rats restores GLUT-2, glucokinase, and glucose-stimulated insulin secretion. *Proc Natl Acad Sci USA* 95: 11921–11926, 1998.
57. **Williams DL, Schwartz MW, Bastian LS, Blevins JE, Baskin DG.** Immunocytochemistry and laser capture microdissection for real-time quantitative PCR identify hindbrain neurons activated by interaction between leptin and cholecystokinin. *J Histochem Cytochem* 56: 285–293, 2008.
58. **Zhang F, Chen Y, Heiman M, Dimarchi R.** Leptin: structure, function and biology. *Vitam Horm* 71: 345–372, 2005.